IEEE Access
Multidisciplinary | Rapid Review | Open Access Journal

Received 8 October 2023, accepted 30 October 2023, date of publication 7 November 2023, date of current version 22 November 2023.

Digital Object Identifier 10.1109/ACCESS.2023.3330743

RESEARCH ARTICLE

A High-Frequency Measurement Method of Downhole Vibration Signal Based on Compressed Sensing Technology and Its Application in Drilling Tool Failure Analysis

FANGXING LYU, YIFAN WANG, YU MEI, AND FEI LI
School of Electronic Engineering, Xi'an Shiyou University, Xi'an, Shaanxi 710065, China
Directional Drilling Laboratory of CNOOC Key Laboratory of Well Logging and Directional Drilling, Xi'an Shiyou University, Xi'an, Shaanxi 710065, China
Corresponding author: Fei Li (lif@xsyu.edu.cn)

This work was supported in part by the National Natural Science Foundation of China under Grant U20B2029 and Grant 52174005, in part by the Key Research and Development Program of Shaanxi under Grant 2022KW-25, in part by the Natural Science Basic Research Plan in Shaanxi Province of China under Grant 2023-JC-YB-453 and Grant 2023-JC-QN-0405, and in part by the Youth Innovation Team of Shaanxi Universities and Shaanxi Province Qinchuangyuan "Scientist+Engineer" Team Construction Plan under Grant 2022kxj-125.

ABSTRACT The high-frequency information of downhole vibration can record more specific details about the dynamic response of bottom hole assembly (BHA), which is conducive to analyzing downhole abnormal vibration and diagnosing drilling tool failure. However, high frequency measurements would generate a large amount of data, which is a huge challenge for data storage. To cope with this challenge, this work proposes applying compressive sensing theory to high-frequency measurement of downhole vibration signals and failure analysis of drilling tools. First, three ADCs clocked at different sub-Nyquist frequencies are used to collect and store downhole vibration signals. Then, the stored sparse vibration data is reconstructed into complete vibration signal by an improved OMP signal reconstruction algorithm. The performance of the proposed method has been investigated via a series of experiments by applying simulation and real vibration signals, which show that the proposed method can reconstruct the downhole vibration signal well and significantly reduce the pressure of acquisition and data storage. This method provides a new way to obtain the high-frequency measurement data of downhole vibration, and provides a data basis for further mastering the comprehensive law of downhole vibration, diagnosing abnormal downhole vibration, and drilling tool failure.

INDEX TERMS Downhole vibration measurement, compressed sensing, drilling tool failure.

I. INTRODUCTION

In the process of drilling, bottom hole assembly (BHA) often encounters serious vibration problems, which will affect the rock-breaking effect, reduce the drilling efficiency, and even lead to drilling tool failure and downhole accidents [1], [2], [3]. The vibration information of BHA is very complex, which includes the vibration of drilling tools themselves, the vibration excited by the interaction between BHA and the formation, and the vibration caused by the collision between BHA and the borehole wall. The vibration signal of BHA is the key to analyzing the real downhole working condition. Also, the measured vibration signals can be used for anomaly detection and fault diagnosis [6], [7], [8]. The theoretical analysis results have some limitations and cannot reflect the real situation of downhole vibration well [4], [5]. Therefore, it is necessary to measure the downhole vibration signal. Generally speaking, the downhole vibration measuring devices

The associate editor coordinating the review of this manuscript and approving it for publication was Fang Yang.

include online upload vibration measuring equipment and offline working micro vibration recorder. In the online upload vibration measuring equipment, the vibration information of BHA collected by the three-axis accelerometer is transmitted to the ground terminal through the mud pulse technology. The disadvantage of these online upload vibration measuring equipment is that the sampling frequency of equipment for downhole vibration is shallow. Only some statistical results, such as the maximum vibration value, can be uploaded due to mud pulse technology's several bits per second transmission speed [9], [10], [11]. Many scholars and drilling companies have recently researched and developed miniaturized offline downhole vibration recorders, such as NOV's BlackBox, Schlumberger's MVC, Baker Hughes's CoPilot, etc. [12], [13], [14]. Most of these miniature vibration recorders are deployed in the modified drilling motor to work offline. They use high-temperature batteries to supply power and independently collect and record downhole vibration signals for several months. Through in-depth analysis of the downhole vibration signals measured by these miniature vibration recorders, it can be found that the high-frequency measurement results of downhole vibration signals can record the dynamic response of downhole drilling tool assemblies in more detail, which is beneficial to the analysis of abnormal downhole vibrations and the diagnosis of drilling tool faults [15], [16], [17], [18]. In 2016, Jeremy summarized the classification of downhole vibration and the corresponding frequency range and discussed the necessity and benefits of the high-frequency vibration measurement [17]. In 2021, Matheus et al. obtained the high-frequency measurement signal of vibration by using the offline downhole vibration measurement method with a sampling frequency of 31250 Hz and conducted the ''ECG'' diagnosis of the downhole vibration signal through the spectrum diagram of the high-frequency measurement data. It was found that these high-frequency data (300 times the frequency of the standard measurement signal) can record more specific details about the dynamic response of the drilling tool, which is beneficial for analyzing and diagnosing abnormal vibration in the well [18]. In 2023, Srivastava et al. discussed sampling frequency of measurements greatly impacts the detection of downhole vibrations. The research results show that high-frequency acquisition helps to clearly observe all the characteristics of the drill string vibration [19], [20], [21]. Downhole vibration measurement equipment needs to work underground for a long time, and the high-frequency detection information of downhole vibration signals generates a large amount of measurement data, which poses a great challenge to the data storage of downhole micro-vibration recorders.

Compressed sensing (CS) theory provides a new promising for solving this kind of problem, which is widely used in analog information converter (AIC), medical CT image compression, image reconstruction and denoising, radar detection, speech recognition, and many other fields [22], [23], [24], [25], [26]. CS theory breaks through the traditional Nyquist sampling theorem's limitations and can reduce the pressure of high-frequency signal acquisition and a large amount of data storage [27], [28]. For vibration signals, Kang et al. have exploited a post-processing scheme to reduce the reconstruction error of CS for structure vibration signals [29]. Chaoyang et al. have proposed a CS method for pump-bearing vibration signals based on the adaptive sparse dictionary model [30]. Qiang et al. have developed an improved CS algorithm for vibration signal processing by taking advantage of the multi-task Bayesian CS and classification theory in the diesel engine health monitoring system [31]. Kato combined a random start uniform sampling method (RSUSM) with CS and apply it to the fault detection of propellers. In the above studies, it is shown that CS technology can be used to compress the vibration data of different equipment, and can perform signal reconstruction and subsequent fault diagnosis [32], [33]. The application of CS theory in vibration signal measurement has involved sparse dictionary representation of vibration signals, optimization of observation matrix, signal reconstruction, and other aspects [34], [35]. However, the research on direct application to downhole vibration signal measurement is still relatively less.

In our previous work, we made a preliminary study on the downhole signals acquiring method using compression sensing technology, however the random modulation of the hardware circuits is complex and not applicable to downhole work [36]. This work uses three low-speed ADCs with different sampling rates to collect and store the downhole vibration signal at the low-frequency region. Then the stored sparse data are used to reconstruct the high-frequency measuring information of downhole vibration signals through the signal recovery algorithm. Compared to high-speed ADC sampling and storage, this sparse data sampling and storing way can significantly reduce the data storage pressure of a miniature vibration recorder. Furthermore, the performance of the proposed method has been investigated via a series of experiments. Therefore, this work may provide good data support for further mastering the comprehensive law of downhole vibration and diagnosing downhole abnormal vibration.

II. SYSTEM CONFIGURATION OF THE PROPOSED METHOD

According to the CS theory, if the measured signal itself or in a transform domain ($\mathbf{\Psi}$ is the sparse basis matrix) is sparse, the high-dimensional signal $V(t)$ can be projected onto a low-dimensional space by constructing an eligible observation matrix $\mathbf{\Phi}$ to obtain the low-dimensional observation signal $\mathbf{Y}$. Then a signal recovery algorithm can be used to reconstruct the measured signal precisely. The system process of the typical CS-based method is shown in **Fig. 1**.

Traditional CS-based method requires the original analog signal to be pre-modulated with a pseudo-random sequence at the Nyquist rate [37]. Different from the traditional CS-based methods, the proposed CS-based method directly samples the information of vibration signal through three parallel ADCs clocked at different sub-Nyquist sampling rates, thereby it can reduce the pressure of massive data storage. The data

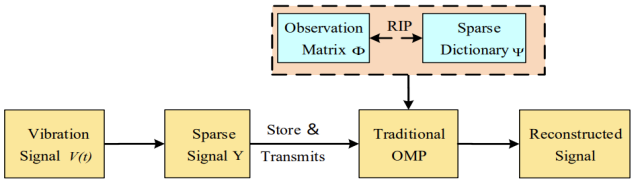

FIGURE 1. The system process of the typical CS-based method.

sampled by one of ADCs is a constant when the frequency of the measured signal is a multiple of one, the recovered signal may have multiple solutions if only by two ADCs, thus three parallel ADCs are used to collect enough information instead of two ADCs. The structure of the proposed method is shown in **Fig. 2**. As can be seen from **Fig. 2**, the downhole vibration signal $V(t)$ is concurrently sampled by three parallel ADCs clocked at the different low sampling rates, and obtain three sampling sequences $V_1(t)$, $V_2(t)$, and $V_3(t)$. The set of these samples is the sparse signal $\mathbf{Y}$. When the downhole vibration recorder finishes its downhole work, the high-frequency downhole vibration signal information can be reconstructed from the observation signal $\mathbf{Y}$ by utilizing the signal recovery algorithm of CS technology.

Parameters N is the number of samples obtained from the high-frequency downhole vibration signal, f_e is the expected high sampling frequency, N_1, N_2 and N_3 are the ratios of f_e to three low-rate ADCs respectively, M_1, M_2 and M_3 are the numbers of samples of three low-rate ADCs respectively, $M$is the total number of samples of three low-rate ADCs.

III. APPLICATION OF CS THEORY IN THE PROPOSED METHOD

The application of CS theory includes the sparse dictionary, the observation matrix, and the signal recovery algorithm. For the downhole vibration signal, the sparse dictionary is the Fourier dictionary, which can be expressed as in (1), shown at the bottom of the page.

From Formula (1), it can be seen that $\mathbf{\Psi_1}$ is composed of N spectral components (also known as N atoms), and the spectral resolution is f_e/N. The observation matrix $\mathbf{\Phi}$ can be constructed through the way of sparse sampling, namely

$$\mathbf{\Phi} = [\boldsymbol{\phi}^T, \boldsymbol{\varphi}^T, \boldsymbol{\gamma}^T]^T \tag{2}$$

where ϕ, φ, and γ are the matrixes of three low-rate ADCs which satisfied the Whittaker–Shannon interpolation, and these matrixes can be expressed as

$$\begin{cases} \phi(m,n) = \text{sinc}c\,(mN_1 - n)\,, 1 \le m \le M_1, 1 \le n \le N \\ \varphi(m,n) = \text{sinc}\,(mN_2 - n)\,, 1 \le m \le M_2, 1 \le n \le N \\ \gamma(m,n) = \text{sinc}\,(mN_3 - n)\,, 1 \le m \le M_3, 1 \le n \le N \end{cases} \tag{3}$$

The essence of the signal recovery algorithm is to find the sparsest expression of the measured signal in the projecting process, and the projection coefficients matrixes are needed to be calculated. The more dictionary atoms, the longer the calculation process takes. However, the more dictionary atoms represent the high spectral resolution of the dictionary, which would be closer to obtaining the sparsest expression of the measured signal. A group of layered dictionaries with $\mathbf{\Psi_1}$ and $\mathbf{\Psi_2}$ is advanced to solve the contradiction between computational complexity and spectral accuracy. $\mathbf{\Psi_2}$ is an ultrahigh spectral resolution dictionary, which can be expressed as in (4), shown at the bottom of the page, where p is the multiple of the spectral resolution coefficient. At last, an improved OMP signal recovery algorithm with layered dictionaries is addressed. The essence of the signal recovery algorithm is to find the sparsest expression of the measured signal. The more dictionary atoms, the longer the calculation process takes. In the improved OMP signal recovery process, $\mathbf{\Psi_1}$ is used to determine the approximate projection range of $\mathbf{\Psi_2}$, and then the corresponding parts of $\mathbf{\Psi_2}$ are used to make the further sparse expression. Thus the total number of atoms in the

$$\Psi_1 = \frac{1}{\sqrt{N}} \begin{bmatrix} 1 & 1 & 1 & \vdots & 1 \\ 1 & e^{j2\pi/N} & e^{j2\pi\times 2/N} & \vdots & e^{j2\pi\times(N-1)/N} \\ \cdots & \cdots & \cdots & \ddots & \cdots \\ 1 & e^{j2\pi\times(N-1)/N} & e^{j2\pi\times 2\times(N-1)/N} & \vdots & e^{j2\pi\times(N-1)\times(N-1)/N} \end{bmatrix} \tag{1}$$

$$\Psi_2 = \frac{1}{N} \begin{bmatrix} 1 & 1 & 1 & \vdots & 1 \\ 1 & e^{j2\pi/(pN)} & e^{j2\pi\times 2/(pN)} & \vdots & e^{j2\pi\times(N-1)/(pN)} \\ \cdots & \cdots & \cdots & \ddots & \cdots \\ 1 & e^{j2\pi\times(pN-1)/(pN)} & e^{j2\pi\times 2\times(pN-1)/(pN)} & \vdots & e^{j2\pi\times(N-1)\times(pN-1)/(pN)} \end{bmatrix} \tag{4}$$

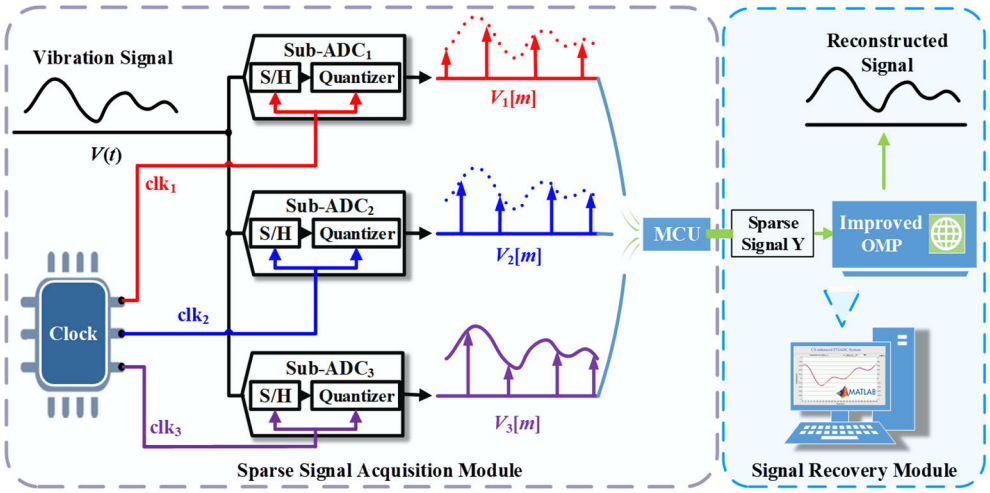

FIGURE 2. The structure of the proposed CS-based method.

calculation process can be greatly reduced, namely

$$\begin{cases} \boldsymbol{Y} = \Phi \times \boldsymbol{V} = \Phi \times \Psi_1 \times \boldsymbol{X}_1 = \boldsymbol{A}_1 \times \boldsymbol{X}_1 (1) \\ \boldsymbol{Y} = \Phi \times \boldsymbol{V} = \Phi \times \Psi_2 \times \boldsymbol{X}_2 = \boldsymbol{A}_2 \times \boldsymbol{X}_2 (2) \end{cases} \tag{5}$$

$\mathbf{A_1}$ and $\mathbf{A_2}$ are sensing matrices with low and spectral resolution, respectively. The flowchart of the proposed improved OMP algorithm is shown in **Fig. 3**.

IV. NUMERICAL SIMULATION AND DRILLING TOOL FAILURE ANALYSIS

A. NUMERICAL SIMULATION

In our work, the value of N is set as 2000. In order to retain the integrity of the measured data information, M should meet the following formula:

$$\boldsymbol{M} \geq 2\boldsymbol{K} \cdot \ln\left(N/K\right) \tag{6}$$

where K is the sparsity of the measured signal. The calculation results of the minimum required sparse samples are shown in **Tab. 1**.

In order to enhance the performance of CS-based method, N_1, N_2 and N_3 are chosen to be co-prime consecutive integers, which should be much bigger than 1. In our work, the values of N_1, N_2 and N_3 are choose as 53, 54 and 55 respectively, the value of M_1, M_2 and M_3 are 37, 37 and 36 respectively, and the value of M is 110. The expected high sampling frequency is set as f_e =5 kS/s, and the sampling rates of low-rate ADCs are $f_1 = f_e$ /53, $f_2 = f_e$ /54 and $f_3 = f_e$ /55 respectively. The multiple of spectral resolution coefficient p is set as 20.

The measured vibration signal is set as multi-frequency components, and its expression can be described as follows:

$$V(t) = \sum_{i=1}^{5} V_i \cos(2\pi f_i t - p_i) \tag{7}$$

where V_i, f_i, and p_i are the corresponding amplitude, frequency, and initial phase of each frequency component,

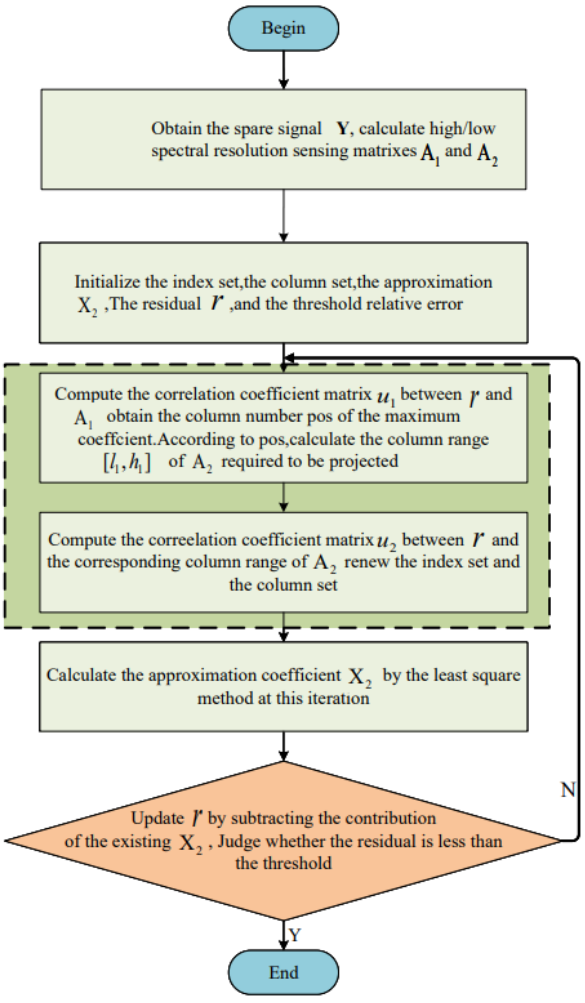

FIGURE 3. The flowchart of the proposed Improved OMP algorithm.

respectively. The number of frequency components is 5, and the amplitude of each frequency component is randomly selected to be 15.7 g, 7.1 g, 8.0 g, 9.5 g, and 5.6 g, respectively.

TABLE 1. Calculation results of minimum sparse sampling points required.

N	K=1	K =2	K =5	K=10	K=20
300	12	21	41	69	109
500	13	23	47	79	129
1000	14	25	53	93	157
2000	16	28	60	106	185

The frequencies of each frequency component are 339.4 Hz, 68.1 Hz, 159.3 Hz, 24.3 Hz, and 6.7 Hz, respectively. The initial phases of each frequency component are $\pi/12$, $\pi/4$, $-\pi/6$, $\pi/3$, and $-\pi/5$, respectively. The waveform of the measured signal and its local amplification are shown in **Fig 4**.

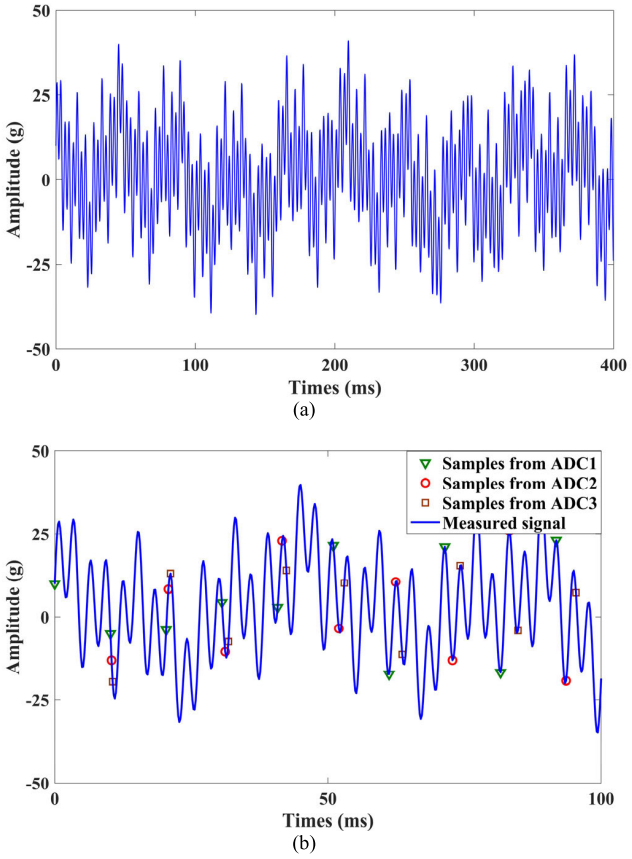

FIGURE 4. The waveform and its local amplification diagram. (a) the waveform of the vibration signal; (b) Locally enlarged view.

B. SIMULATION RESULT AND DISCUSSION

According to the layered dictionaries described above, an indexed dictionary $\mathbf{\Psi_1}$ and a fine dictionary $\mathbf{\Psi_2}$ with high spectral resolution are constructed. $\mathbf{\Psi_1}$ has 2000 atoms, and the length of each atom is 2000. It contains a spectral range of 0∼5 kHz, and the spectral resolution is 5 kHz/2000=2.5 Hz. $\mathbf{\Psi_2}$ has 40000 atoms, and the length of each atom is 2000, and the spectral resolution is 5 kHz/40000=0.125 Hz. The observation matrix $\mathbf{\Phi}$ is established through Formula (2), whose size is 110×2000. The samples of two low-rate ADCs are re-sequenced to form the sparse signal $\mathbf{Y}$, which is shown in **Fig 5**. Then the improved OMP recovery algorithm is used to obtain the measured signal at an expected high sampling rate. The sensing matrices $\mathbf{A_1}$ and $\mathbf{A_2}$ with the low and spectral resolution are Calculated by utilizing Formula (5).

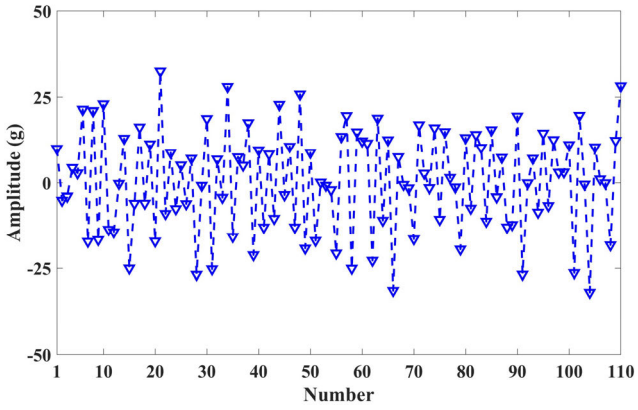

FIGURE 5. The samples of sparse signal.

At the first iteration, the projection result of residual signal $\mathbf{r}$ on $\mathbf{A}_1$ is shown in **Fig. 6(a)**. From **Fig. 6(a)**, it can be seen that the maximum projection coefficient on $\mathbf{A_1}$ is column 137, and it can be calculated that the corresponding projection range of $\mathbf{A_2}$ is column 2700∼2740. The projection result of $\mathbf{r}$ on columns 2700 ∼2740 of $\mathbf{A_2}$ are shown in **Fig. 6(b)**. It can be seen from **Fig. 6(b)** that the maximum projection coefficient of $\mathbf{A_2}$ is column 2716. Therefore, the atom of $\mathbf{\Psi_2}$ that best matches the measured signal at the first iteration is the 2716th atom, which indicates that the corresponding frequency of 339.375 Hz best represents the measured signal found in the first iteration. Then the 2716th atom is added to the support set to update $\mathbf{r}$, and the result is shown in **Fig. 6(c)**. The above process is repeated until the modulus of $\mathbf{r}$ is below the set threshold, and an atom that best represents the measured signal is searched for to update $\mathbf{r}$ at each iteration. The relative error of $\mathbf{r}$ with iteration times is shown in **Fig. 6(d)**.

Finally, the approximation $\mathbf{X}_2^{\#}$ of $\mathbf{X_2}$ is obtained, and the reconstructed waveform is shown in **Fig. 7**. It can be seen from **Fig. 7(b)** that the time interval between two adjacent nodes of the reconstructed waveform is 0.2 ms, which indicates that the expected high sampling rate reaches 5 kS/s. The error of the reconstructed signal obtained by the proposed method is 2.17% after 11th iteration. Randomly change the frequency, amplitude and initial phase of the signal, and repeat the above simulation process over 200 times. The simulation results show that the average reconstructed error is ∼2.61%, which means a good reconstructed effect by the proposed method. The value of N and M are 2000 and 110 respectively, hence the compression ratio of the proposed method is 18.2.

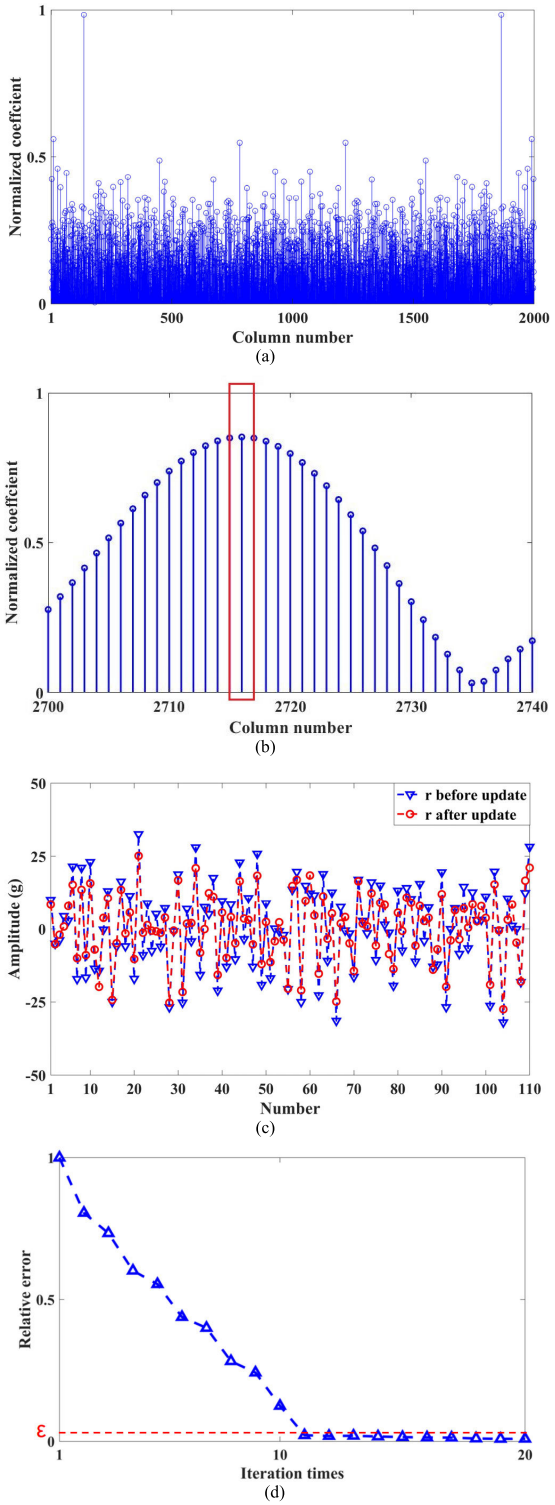

FIGURE 6. Reconstructed process of the measured signal. (a) The projection of r on A1 at the first iteration; (b) The projection result of r on corresponding projection range of A2 at the first iteration; (c) r before and after update at the first iteration; (d) Relative error of r varies with iteration times.

C. RECONSTRUCTED OF VIBRATION SIGNAL AND DRILLING TOOL FAILURE ANALYSIS

In order to further demonstrate the reconstruction effect of the proposed method, the data collected in the laboratory

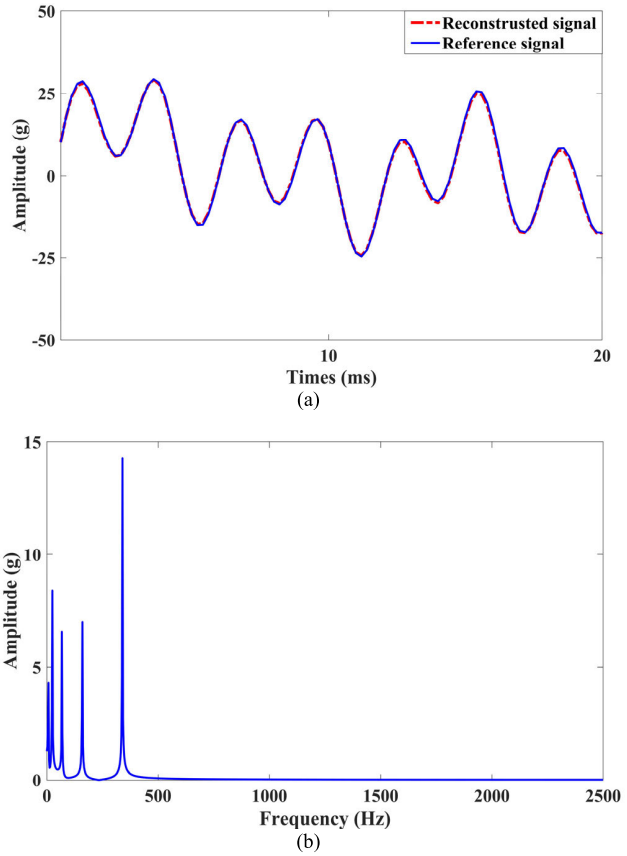

FIGURE 7. The local waveform and frequency spectrum of the reconstructed signal. (a) Local enlarge waveform; (b) frequency spectrum of the reconstructed signal.

vibration table testing and cement target testing are used. The reconstructed processes of these signals are the same as that of the simulation signal. The laboratory test environment is shown in **Fig. 8**, and the vibration data acquisition module is fixed on the vibration table for laboratory testing. **Fig. 9** is a typical set of the reconstructed and the reference waveforms of the laboratory test. The vibration frequency of the laboratory test is 50 Hz, and the amplitude is 20 g. The reconstruction signal error obtained by the proposed method is ∼7.44%.

Fig. 10 is a typical set of the reconstructed and the reference waveforms of the cement target testing collected by the vibration data acquisition module. The reconstruction signal error obtained by this method is ∼14.58%. Compared with the recovery effect of the simulated signal, the recovery effect of the actual vibration signal is worse. The reason is that the actual vibration signal is complex and contains noise components, which cannot be sparsely represented by Fourier dictionary. In the reconstructed process of the cement target testing, we can calculate that the atoms of $\Psi 2$ best matches the measured signal are the 1th atom, 18th atom, 105th atom, 1075th atom, 1466th atom and 294th atom, which indicates that the corresponding frequency of 0 Hz, 2.125 Hz, 13 Hz, 134.25 Hz, 183.25 Hz, and 36.625 Hz, and the frequency spectrum of the reconstructed signal is shown in Fig. 11.

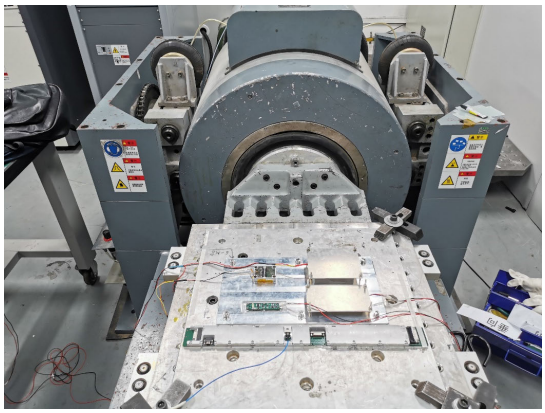

FIGURE 8. Photo of laboratory test environment.

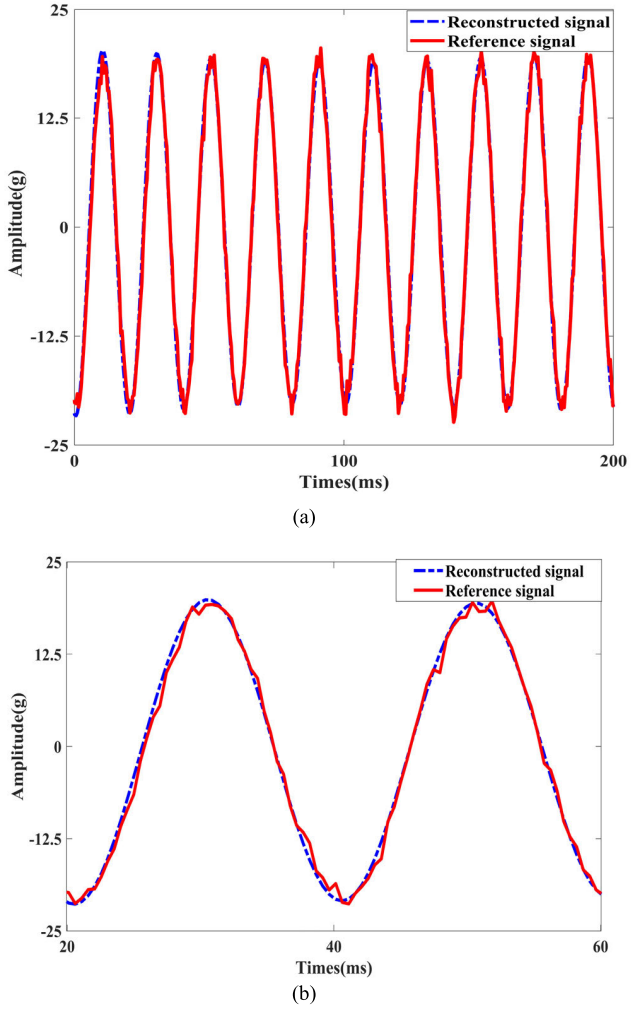

FIGURE 9. Reconstruction effect and local amplification of vibration waveform under laboratory shaking table test (a) Waveform of the reconstructed signal; (b) Locally enlarged view.

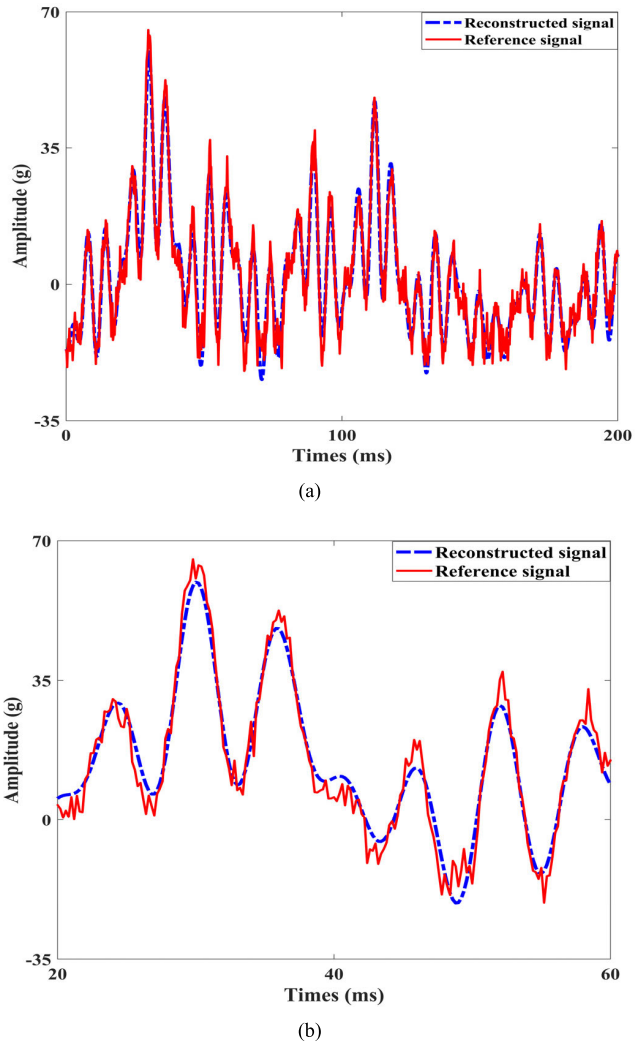

FIGURE 10. Waveform reconstruction effect and local amplification of the cement target testing vibration signal. (a) Waveform of the reconstructed downhole signal; (b) Locally enlarged view.

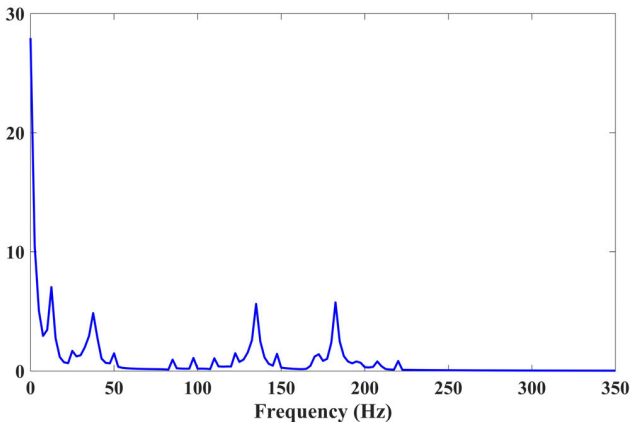

FIGURE 11. Frequency spectrum of the reconstructed actual drilling vibration signal.

Also, the time domain and frequency domain characteristics of the main vibration signal can be obtained in the reconstructed process. From the time domain waveform of the reconstructed vibration signal, we can obtain the maximum value of vibration amplitude and some statistical information for a certain amplitude range. From the frequency

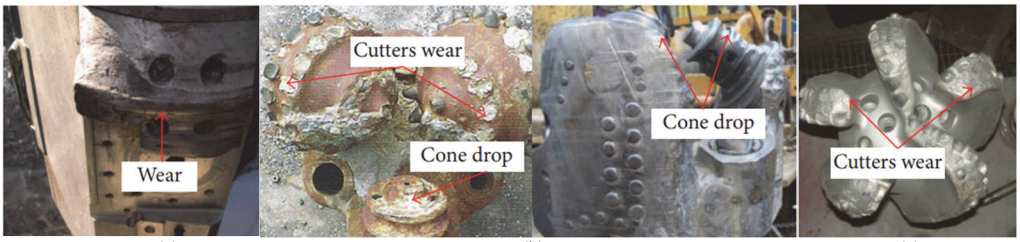

FIGURE 12. Photo of different drilling tool failure. (a) MWD tool failure; (b) Tricone bit failure; (c) PDC bit failure.

TABLE 2. Main characteristics of different forms of downhole vibration signal.

Forms	Frequency (Hz)	Amplitude (g)	Tool damage
Stick-slip	0.1~5	0~10	PDC bit damaged, drill string twist off or washout
Bit-bounce	1~10	0~100	Bit damaged and BHA washout
Bit whirl	10~50	0~200	Cutter and/or stabilizers damaged, increase torque
BHA whirl	5~20	0~100	Cutter and/or stabilizers damaged, increase torque
Lateral shock	1~5	0~14	BHA washout
Torsional resonance	20~350	/	Cutter and/or stabilizers damaged, increase torque
Parametric resonance	0.1~10	/	Cutter and/or stabilizers damaged, increase torque
Bit chatter	20~250	/	Bit damage, BHA washout
VIV	0.1~20	/	Riser damage
Modal coupling	0.1~350	/	Drill string twist off

spectrum of the reconstructed of the reconstructed vibration signal, we can obtain the main frequencies and corresponding vibration amplitudes.

As classified by the past study [13], the frequencies, amplitudes response, and tool damage of different forms of downhole vibration signal is listed in **Tab. 2**. From **Tab. 2**, we can see that the main characteristics (such as frequency and amplitude range) of different forms of downhole vibration signal of different forms of downhole vibration signal are different, and their damage to drilling tools is different (as shown in **Fig. 12**). Among them, only Torsional resonance, Bit chatter and Modal coupling have the high frequency components greater than 50 Hz, and the maximum frequency and amplitude of different forms vibration are 350 Hz and 200 g respectively. Combined with some key information such as the time domain and frequency domain characteristics of the downhole vibration signal and the different operating conditions of drilling tool, the failure degree and early warning of the drilling tool may be judged. This method can make the drilling tool fault diagnosis pay more attention to the characteristics of high-frequency signals, while the existing methods pay more attention to the characteristics of middle and low-frequency signals due to the limitation of sampling frequency. Also, improper drilling operations and improper drilling tool protection measures may lead to drilling tool failure, so we need to avoid such cases [38], [39].

V. CONCLUSION

A high-frequency measurement method of downhole vibration based on compressed sensing technology is proposed. This method provides a promising way to acquire the high-frequency measurement data of downhole vibration, which may be helpful for the analysis and extraction of downhole working condition information. The results show that the proposed method can greatly reduce the pressure for the massive storage of downhole high-frequency signals, and the compression ratio is 18.2. The time domain and frequency domain characteristics and information statistics results of reconstructed vibration data can be used to predict the failure degree of drilling tools, so as to avoid the occurrence of drilling accidents. Moreover, the field test will be the next step of the project team's work plan.

REFERENCES

[1] T. Feng, S. Bakshi, Q. Gu, Z. Yan, and D. Chen, "Design optimization of bottom-hole assembly to reduce drilling vibration," *J. Petroleum Sci. Eng.*, vol. 179, pp. 921–929, Aug. 2019, doi: 10.1016/j.petrol.2019.04.107.

[2] H. Zhang, Q. Di, W. Wang, F. Chen, and W. Chen, "Lateral vibration analysis of pre-bent pendulum bottom hole assembly used in air drilling," *J. Vibrat. Control*, vol. 24, no. 22, pp. 5213–5224, Nov. 2018, doi: 10.1177/1077546317747778.

[3] R. G. Oliveira, L. F. Almeida, J. G. L. Lazo, A. G. Manhaes, and M. F. Pinto, "Smart oil field management system using evolutionary intelligence," *IEEE Access*, vol. 11, pp. 45798–45814, 2023, doi: 10.1109/ACCESS.2023.3272335.

[4] B. Li, Y. Gao, and R. Li, "Research and analysis of drilling string vibration signals," in *Proc. IEEE Int. Conf. Mechatronics Autom. (ICMA)*, Oct. 2020, pp. 12–17, doi: 10.1109/ICMA49215.2020.9233640.

[5] Y. Hou, R. Zhou, X. Long, P. Liu, and Y. Fu, "The design and simulation of new downhole vibration device about acoustic oil recovery technology," *Petroleum*, vol. 1, no. 3, pp. 257–263, Sep. 2015, doi: 10.1016/j.petlm.2015.09.001.

[6] G. Madhukar, S. Boosi, Z. A. Adhoni, K. A. Bhaskar, and A. V. Naik, "A machine learning based methodology for fault diagnosis in rotating machine," in *Proc. IEEE Int. Conf. Integr. Circuits Commun. Syst. (ICICACS)*, Feb. 2023, pp. 1–5, doi: 10.1109/ICICACS57338.2023.10100301.

[7] M. Civera and C. Surace, "Instantaneous spectral entropy: An application for the online monitoring of multi-storey frame structures," *Buildings*, vol. 12, no. 3, p. 310, Mar. 2022, doi: 10.3390/buildings12030310.

[8] M. Civera and C. Surace, "An application of instantaneous spectral entropy for the condition monitoring of wind turbines," *Appl. Sci.*, vol. 12, no. 3, p. 1059, Jan. 2022, doi: 10.3390/app12031059.

[9] R. L. Cook, J. W. Nicholson, M. C. Sheppard, and W. Westlake, "First real time measurements of downhole vibrations, forces, and pressures used to monitor directional drilling operations," in *Proc. SPE/IADC Drilling Conf. Exhib.*, Feb. 1989, p. 18651, doi: 10.2118/18651-MS.

[10] S. Mahalungkar and M. Ingram, "Online and manual (offline) vibration monitoring of equipment for reliability centered maintenance," in *Proc. IEEE-IAS/PCA Cement Ind. Tech. Conf.*, Jul. 2004, pp. 245–261, doi: 10.1109/CITCON.2004.1309871.

[11] D. I. Qinfeng, P. Junchao, L. I. Ning, W. Wenchang, W. Mingjie, and Z. He, "Progress in measurement technology for drill string vibration," *Mech. Eng.*, vol. 37, no. 5, pp. 565–579, Oct. 2015, doi: 10.6052/1000-0879-15-044.

[12] I. Kessai, S. Benammar, M. Z. Doghmane, and K. F. Tee, "Drill bit deformations in rotary drilling systems under large-amplitude stick-slip vibrations," *Appl. Sci.*, vol. 10, no. 18, p. 6523, Sep. 2020, doi: 10.3390/app10186523.

[13] G. Dong and P. Chen, "A review of the evaluation, control, and application technologies for drill string vibrations and shocks in oil and gas well," *Shock Vibrat.*, vol. 2016, pp. 1–34, Oct. 2016, doi: 10.1155/2016/7418635.

[14] F. Li, "Vibration of drilling motors in unconventional oil and gas exploration with a miniature recorder," *J. Eng.*, vol. 2020, no. 2, pp. 79–85, Feb. 2020, doi: 10.1049/joe.2019.1130.

[15] H. Oueslati, J. R. Jain, H. Reckmann, L. W. Ledgerwood, R. Pessier, and S. Chandrasekaran, "New insights into drilling dynamics through high-frequency vibration measurement and modeling," in *Proc. SPE Annu. Tech. Conf. Exhib.*, Sep. 2013, pp. 166–212, doi: 10.2118/166212-MS.

[16] J. Tian, C. Fan, T. Zhang, and Y. Zhou, "Rock breaking mechanism in percussive drilling with the effect of high frequency torsional vibration," *Energy Sour., A, Recovery, Utilization, Environ. Effects*, vol. 44, no. 1, pp. 2520–2534, Mar. 2022, doi: 10.1080/15567036.2019.1650138.

[17] J. A. Greenwood, "Vibration monitoring and mitigation—An integrated measurement system," in *Proc. SPE/IADC Drilling Conf. Exhib.*, Mar. 2016, pp. 178–773, doi: 10.2118/178773-MS.

[18] J. Matheus, M. Ignova, and D. Amaya, "A medical-inspired framework to classify downhole shocks waveforms while drilling," in *Proc. SPE/IADC Int. Drilling Conf. Exhib.*, Mar. 2021, pp. 098–204, doi: 10.2118/204098-MS.

[19] S. Srivastava, A. Sharma, and C. Teodoriu, "Optimizing sampling frequency of surface and downhole measurements for efficient stick-slip vibration detection," *Petroleum*, Feb. 2023, Art. no. S2405656123000135, doi: 10.1016/j.petlm.2023.02.004.

[20] T. Townsend, W. Moss, D. Heinisch, K. Evans, and C. Schandorf, "Advanced high frequency in-bit vibration measurement including independent, spatially separated sensors for proper resolution of vibration components including lateral, radial, and tangential acceleration," in *Proc. Int. Petroleum Exhib. Conf.*, Dec. 2021, pp. 110–208, doi: 10.2118/208110-MS.

[21] S. Jones and J. Sugiura, "Analysis of surface and downhole drilling dynamics high-frequency measurements enhances the prediction of downhole drilling dysfunctions and improves drilling efficiency," in *Proc. Int. Petroleum Exhib. Conf.*, Nov. 2020, pp. 202–859, doi: 10.2118/202859-MS.

[22] G. Zhou, Y. Qi, Z. H. Lim, and G. Zhou, "Single-pixel MEMS spectrometer based on compressive sensing," *IEEE Photon. Technol. Lett.*, vol. 32, no. 5, pp. 287–290, Mar. 1, 2020, doi: 10.1109/LPT.2020.2970742.

[23] H. Ding, F. Lyu, H. Zhao, X. Niu, and C. Han, "Sub-Nyquist sampling method and its application in high-frequency electric-field measurement," *Opt. Eng.*, vol. 58, no. 11, Nov. 2019, Art. no. 114106, doi: 10.1117/1.OE.58.11.114106.

[24] V. K. Amalladinne, J. R. Ebert, J.-F. Chamberland, and K. R. Narayanan, "An enhanced decoding algorithm for coded compressed sensing with applications to unsourced random access," 2021, *arXiv:2112.00270*.

[25] Y. Li, Y. Jiang, H. Zhang, J. Liu, X. Ding, and G. Gui, "Nonconvex $L_{1/2}$—Regularized nonlocal self-similarity denoiser for compressive sensing based CT reconstruction," *J. Franklin Inst.*, vol. 360, no. 6, pp. 4172–4195, Apr. 2023, doi: 10.1016/j.jfranklin.2023.01.041.

[26] Y. Li, L. Gao, S. Hu, G. Gui, and C.-Y. Chen, "Nonlocal low-rank plus deep denoising prior for robust image compressed sensing reconstruction," *Exp. Syst. Appl.*, vol. 228, Oct. 2023, Art. no. 120456, doi: 10.1016/j.eswa.2023.120456.

[27] D. L. Donoho, "Compressed sensing," *IEEE Trans. Inf. Theory*, vol. 52, no. 4, pp. 1289–1306, Apr. 2006, doi: 10.1109/TIT.2006.871582.

[28] Y. Bo, X. Qing, Y. Shuna, and C. Hao, "Wideband sparse signal acquisition with ultrahigh sampling compression ratio based on continuous-time photonic time stretch and photonic compressive sampling," *Appl. Opt.*, vol. 61, no. 6, pp. 1344–1348, 2022, doi: 10.1364/AO.450386.

[29] J. Kang, W. Ren, Y.-L. Xie, Y. Zhao, and J.-F. Wang, "An enhanced method to reduce reconstruction error of compressed sensing for structure vibration signals," *Mech. Syst. Signal Process.*, vol. 183, Jan. 2023, Art. no. 109585, doi: 10.1016/j.ymssp.2022.109585.

[30] X. Chaoang, T. Hesheng, and R. Yan, "Compressed sensing reconstruction for axial piston pump bearing vibration signals based on adaptive sparse dictionary model," *Meas. Control*, vol. 53, nos. 3–4, pp. 649–661, Jan. 2020, doi: 10.1177/0020294019898725.

[31] W. Qiang, Z. Peilin, M. Chen, W. Huaiguang, and W. Cheng, "Multi-task Bayesian compressive sensing for vibration signals in diesel engine health monitoring," *Measurement*, vol. 136, pp. 625–635, Mar. 2019, doi: 10.1016/j.measurement.2018.07.074.

[32] Y. Kato, "Fault diagnosis of a propeller using sub-nyquist sampling and compressed sensing," *IEEE Access*, vol. 10, pp. 16969–16976, 2022, doi: 10.1109/ACCESS.2022.3149756.

[33] X. Tang, Y. Xu, X. Sun, Y. Liu, Y. Jia, F. Gu, and A. D. Ball, "Intelligent fault diagnosis of helical gearboxes with compressive sensing based non-contact measurements," *ISA Trans.*, vol. 133, pp. 559–574, Feb. 2023, doi: 10.1016/j.isatra.2022.07.020.

[34] I. Ahmed, A. Khalil, I. Ahmed, and J. Frnda, "Sparse signal representation, sampling, and recovery in compressive sensing frameworks," *IEEE Access*, vol. 10, pp. 85002–85018, 2022, doi: 10.1109/ACCESS.2022.3197594.

[35] S. Thiruppathirajan, S. Sreelal, and B. S. Manoj, "Sparsity order estimation for compressed sensing system using sparse binary sensing matrix," *IEEE Access*, vol. 10, pp. 33370–33392, 2022, doi: 10.1109/ACCESS.2022.3161523.

[36] F. Lyu, Y. Li, Y. Zhang, X. Fang, F. Li, and C. Hu, "Downhole vibration acquisition method based on compressed sensing technology," in *Proc. 4th Int. Conf. Intell. Control, Meas. Signal Process. (ICMSP)*, Jul. 2022, pp. 460–464, doi: 10.1109/ICMSP55950.2022.9859126.

[37] S. Qaisar, R. M. Bilal, W. Iqbal, M. Naureen, and S. Lee, "Compressive sensing: From theory to applications, a survey," *J. Commun. Netw.*, vol. 15, no. 5, pp. 443–456, Oct. 2013, doi: 10.1109/JCN.2013.000083.

[38] S. M. Zamani, S. A. Hassanzadeh-Tabrizi, and H. Sharifi, "Failure analysis of drill pipe: A review," *Eng. Failure Anal.*, vol. 59, pp. 605–623, Jan. 2016, doi: 10.1016/j.engfailanal.2015.10.012.

[39] B. Liu, Z. Zhu, J. Zhang, W. Lei, and B. Wu, "Fatigue failure analysis of drilling tools for ultra-deep wells in Shunbei block," *IOP Conf. Ser., Mater. Sci. Eng.*, vol. 423, Nov. 2018, Art. no. 012190, doi: 10.1088/1757-899X/423/1/012190.

FANGXING LYU received the B.S., M.S., and Ph.D. degrees in measurement and instrumentation from Xi'an Jiaotong University, Xi'an, China, in 2007, 2010, and 2020, respectively. Since 2021, he has been a Lecturer with Xi'an Shiyou University. He is the author of two books, more than 20 articles, and six inventions. His current research interests include compressed sensing technology, optical fiber sensing technology, and directional drilling technology.

YIFAN WANG is currently pursuing the M.S. degree with Xi'an Shiyou University, China. He is good at Python data analysis. His current research interests include data analysis, compressed sensing, and deep learning.

YU MEI received the B.S. degree in electronic information engineering from Xi'an Shiyou University, in 2021, where she is currently pursuing the M.Sc. degree in instrument science and technology. Her research interests include attitude measurement while drilling, research on related model construction, and system simulation testing.

FEI LI received the B.S. and M.S. degrees in measurement and instrumentation from Xi'an Jiaotong University, Xi'an, China, in 2000 and 2003, respectively, and the Ph.D. degree in electronic and electrical engineering from the University of Strathclyde, U.K., in 2006. Since 2018, he has been a Professor with Xi'an Shiyou University. He is also the Director of the Directional Drilling Laboratory of CNOOC Key Laboratory of Well Logging and Directional Drilling. He is the author of three books, more than 30 articles, and 20 inventions. His current research interests include drilling automation technology and directional drilling technology.